



Published in final edited form as:

*J Magn Reson Imaging*. 2012 May ; 35(5): 1222–1226. doi:10.1002/jmri.23571.

## Improved $B_1$ Homogeneity of 3 Tesla Breast MRI Using Dual-Source Parallel Radiofrequency Excitation

Habib Rahbar, MD<sup>1</sup>, Savannah C. Partridge, PhD<sup>1</sup>, Wendy B. DeMartini, MD<sup>1</sup>, Robert L. Gutierrez, MD<sup>1</sup>, Sana Parsian, MD<sup>1</sup>, and Constance D. Lehman, MD, PhD<sup>1</sup>

<sup>1</sup>Department of Radiology, University of Washington, Seattle Cancer Care Alliance, 825 Eastlake Avenue East, Seattle, WA 98109-1023

### Abstract

**Purpose**—To compare breast MRI  $B_1$  homogeneity at 3 Tesla with and without dual-source parallel radiofrequency (RF) excitation.

**Materials and Methods**—After institutional review board approval, we evaluated 14 consecutive breast MR examinations performed at 3 Tesla that included 3D  $B_1$  maps created separately with conventional single-source and dual-source parallel RF excitation techniques. We measured  $B_1$  values (expressed as % of intended  $B_1$ ) on each  $B_1$  map at nipple level in multiple bilateral locations: anterior, lateral, central, medial, and posterior. Mean whole breast and location specific  $B_1$  values were calculated and compared between right and left breasts using paired t-test.

**Results**—Mean whole breast  $B_1$  values differed significantly between right and left breasts with standard single-source RF excitation (difference L-R,  $\Delta=9.2\%$ ;  $p<0.001$ ) but not with dual-source parallel RF excitation ( $\Delta=2.3\%$ ;  $p=0.085$ ). Location specific  $B_1$  values differed significantly between right and left on single-source in the lateral ( $p=0.014$ ), central ( $p=0.0001$ ), medial ( $p=0.0013$ ), and posterior ( $p<0.0001$ ) locations. Conversely, mean  $B_1$  values differed significantly on dual-source parallel RF excitation for only the anterior ( $p=0.030$ ) and lateral ( $p=0.0003$ ) locations.

**Conclusion**— $B_1$  homogeneity is improved with dual-source parallel RF excitation on 3T breast MRI when compared to standard single-source RF excitation technique.

### Introduction

The use of magnetic resonance imaging (MRI) at 3 Tesla (T) has increased substantially in recent years. This increase in field strength over the more commonly used 1.5T scanners provides higher signal to noise (SNR), leading to potential benefits including greater spatial resolution and decreased scan times. Despite these advantages, MRI at 3T also creates significant technical challenges. Chief among these, particularly in breast imaging, is tissue signal variability or “shading” due to  $B_1$  transmit field inhomogeneity resulting from dielectric resonance effects.

First reported in breast MRI by Kuhl et al (1) and further quantitatively described by Azlan et al (2), these adverse  $B_1$  effects are due to the higher frequency  $B_1$  transmit fields that are used at greater field strengths. This results in non-uniform flip angles and measured signal, most pronounced from right-to-left for bilateral axial breast imaging (3). The non-uniformity can lead to significant variations in T1 contrast that in turn cause significant

Address Correspondence To: Habib Rahbar, MD, Acting Assistant Professor of Radiology, University of Washington School of Medicine, Seattle Cancer Care Alliance, 825 Eastlake Ave. E., G3-200, Seattle, WA 98109-1023, Phone: 206-288-6241, Fax: (206) 288-6473, hrahbar@uw.edu.

spatial variations in signal intensity and contrast-enhancement or variations in fat saturation uniformity for non-adiabatic radiofrequency (RF) pulses. This resulting tissue contrast and signal enhancement inhomogeneity is particularly problematic in dynamic contrast-enhanced (DCE) breast MRI.

Proposed solutions to address the issue of tissue shading effects include techniques to maximize T1 contrast, including 3D imaging and increased flip angles (3,4). Recently, dual-source parallel excitation techniques have been developed to address the challenge of dielectric shading by increasing uniformity of the applied RF field. The use of independent transmit channels also allows for optimization of the local and whole-body specific energy absorption rate (SAR) using patient adaptive techniques, leading to reduced SAR deposition levels and decreased scan times (5). This technique has been shown to be useful in body and musculoskeletal imaging (5,6), but to date there are no published studies examining its effectiveness in reducing B<sub>1</sub> inhomogeneities in breast MRI at 3T. We thus sought to evaluate MRI B<sub>1</sub> homogeneity in breast imaging at 3T with and without dual-source parallel RF excitation.

## Methods

### Patient Population

The protocol for this study was approved by our institutional review board and was compliant with the Health Insurance Portability and Accountability Act. Our institutional review board waived informed consent. We included 15 consecutive patients who underwent a clinical breast MRI from February 18, 2010 to March 8, 2010. Several patient body composition factors were assessed. Patient height, weight, and body-mass-index were obtained from the medical records. Breast size was visually assessed for each patient by examining the B<sub>1</sub> maps at the level of the nipple and categorized as small, medium, or large while also noting any asymmetry.

### B<sub>1</sub> Maps Acquisition

All MR examinations were performed on a Philips Achieva Tx 3T scanner using a dedicated 16-channel bilateral breast coil (Philips Healthcare, Best, the Netherlands). Patients were scanned axially in the prone position with feet first. After the standard clinical breast MRI sequences were obtained (including a T2-weighted fast spin echo sequence, T1-weighted non-fat suppressed sequence, and a T1-weighted fat-suppressed dynamic contrast-enhanced MRI sequence), B<sub>1</sub> transmission field mapping was performed separately with conventional single-source RF excitation and dual-source parallel RF excitation (MultiTransmit, Philips Healthcare, Best, the Netherlands) techniques (7).

As previously described (6), the dual-source parallel RF excitation technique employed in our study distributes RF power to the ports of the system body coil using two independent RF transmit channels under full software control. The resulting applied B<sub>1</sub> field is effectively a linear combination of the B<sub>1</sub> fields generated by each source. Using patient-adaptive RF shimming, the power, amplitude, phase and waveform of the two RF sources are automatically adjusted for optimal uniformity in each patient's unique anatomy. In practice, the process involves first acquiring a short B<sub>1</sub> calibration scan on a per-patient basis to map the B<sub>1</sub> field produced in the subject by each of the independent RF sources and determine the expected RF energy deposition in the patient. For breast imaging, parallel RF excitation can be used during particular acquisitions (by selecting it in the protocol) to improve B<sub>1</sub> homogeneity, without requiring changes to other sequence parameters.

For our study, B<sub>1</sub> maps were calculated using both standard single-source and parallel dual-source RF excitation. In each case, optimal B<sub>0</sub> homogeneity was first achieved using a

patient-adaptive image-based  $B_0$  shimming technique (SmartExam Breast, Philips Healthcare, Best, The Netherlands). Next,  $B_1$  transmission field maps were created using a previously described actual flip-angle imaging (AFI) approach (2,7), which enables accurate and rapid 3D in vivo measurement of the  $B_1$  field. This method employs a 3D gradient echo pulse sequence incorporating two identical RF pulses but with different TRs, and imaging parameters were defined based on previous recommendations (2,7):  $TR_1/TR_2 = 30/150$  msec,  $TE = 2.2$  msec, flip angle =  $60^\circ$ , matrix size =  $128 \times 128$ , FOV =  $40 \times 40$  cm, slice thickness = 12 mm, and number of slices = 7. The same imaging parameters were used for standard single-source and dual-source RF excitation acquisitions. A  $B_1$  calibration scan was run prior to the dual-source RF excitation acquisition, as described above.

### Image Measurements

$B_1$  maps were calculated by measuring the actual flip angles generated in the subject relative to the intended flip angle, expressed as a percentage, using the relationship:

$$\alpha \approx \cos^{-1} \frac{rn - I}{n - r} \quad (1)$$

where  $\alpha$  is the actual flip angle,  $r$  is the signal ratio  $S_1/S_2$  with  $S_1$  and  $S_2$  the signals measured after the corresponding TRs ( $TR_1=30$ msec,  $TR_2=150$ msec),  $n = TR_2/TR_1$ . Profile plots were defined on  $B_1$  maps to quantify right to left variation across the field of view using ImageJ (National Institute of Health, Bethesda, MD).  $B_1$  values were measured by defining five circular regions of interest (ROIs) of equal area ( $1.2 \text{ cm}^2$ ) in each breast on each  $B_1$  map at the level of the nipple. ROIs were drawn for each subject in the following bilateral locations: anterior, lateral, central, medial, and posterior (figure 1). Mean whole breast  $B_1$  values were also calculated for each subject by averaging the five ROI values for each breast.

### Statistical Analysis

Intra-patient differences between right and left whole breast and location-specific  $B_1$  values for both dual-source parallel RF and single-source RF excitation techniques were evaluated using paired t-test. All computations were performed using JMP version 9.0.2 (SAS Institute Inc, Cary, NC).

### Results

We scanned 15 patients with both single-source and dual-source parallel RF excitation techniques. A single patient who had undergone left mastectomy with silicone breast implant reconstruction was excluded ( $n=1$ ) due to inability to draw ROIs of left breast tissue. Thus, the final cohort included 14 patients. Indications for the clinical breast MRI in the study patients were high risk screening ( $n=7$ ), evaluation of extent of disease in patients with known breast cancer ( $n=6$ ), and short-interval 6 month follow-up for a prior MRI finding in a high risk screening patient ( $n=1$ ). The mean patient age was 55 years.

The patient cohort exhibited varied body compositions, with a relatively even distribution of breast sizes (small  $n=5$  patients, medium  $n=6$  patients, large  $n=3$  patients). Only one patient demonstrated visually perceptible breast size asymmetry (right breast was larger than the left). Mean patient height was  $164.6 \pm 6.8$  cm, mean patient weight was  $69.9 \pm 9.2$  kg, and mean patient body-mass-index was  $25.4 \pm 2.8$  cm/kg.

## Whole Breast $B_1$ Values and Comparisons

$B_1$  measures are reported in Table 1. Mean whole breast  $B_1$  values per patient ranged from 72 – 108% (median, 90%) for single-source RF excitation technique and 90 – 116% (median, 102%) for dual-source parallel RF excitation technique. Mean right whole breast  $B_1$  values differed significantly from mean left whole breast  $B_1$  values with single-source RF excitation (mean difference L-R,  $\Delta=9.2\%$ ;  $p<0.001$ ) but not with dual-source parallel RF excitation (mean difference L-R,  $\Delta=2.3\%$ ;  $p=0.085$ ) (figure 2). An example comparing the variations in  $B_1$  values between the right and left breast with conventional single-source and dual-source parallel RF excitation techniques in a single patient is provided in figure 3.

## Regional $B_1$ Values and Comparisons

Intra-patient regional  $B_1$  values significantly differed between right and left on single-source RF excitation in the lateral ( $p=0.014$ ), central ( $p=0.0001$ ), medial ( $p=0.0013$ ), and posterior ( $p<0.0001$ ) locations, with posterior regions demonstrating the greatest  $B_1$  inhomogeneities ( $\Delta=-14\%$ ). Conversely, mean  $B_1$  values differed significantly on dual-source parallel RF excitation for only the anterior ( $p=0.030$ ) and lateral ( $p=0.0003$ ) locations, Table 1.

## Discussion

Single-source RF transmission attempts to generate a circularly polarized RF field by utilizing a single RF source that is split between two ports  $90^\circ$  apart. This design, termed quadrature drive or mode, was adequate at 1.5T and lower magnetic ( $B_0$ ) field strengths. However, at 3T field strength, standing wave effects are more problematic, particularly in larger patients, resulting in non-uniform RF excitation across the field of view. Recently, several studies have demonstrated that the use of multiple channels with parallel RF excitation can substantially improve image homogeneity in both body and musculoskeletal imaging applications (5,6,8–10). However, there are currently no published studies that specifically examine the use of this novel technique for the breast imaging application, where  $B_1$  inhomogeneities are particularly problematic due to off-center positioning of patients' breasts in the whole-body RF coil (2).

The system utilized in our study enables the use of both single-source RF excitation and dual-source excitation within the body coil, allowing for our intra-examination comparisons. We demonstrated that there is improvement in  $B_1$  homogeneity with dual-source parallel RF excitation techniques on 3D breast MRI when compared to the conventional single-source technique. For whole breast averaged  $B_1$  measures, there were significant right-to-left differences on single-source RF excitation maps, but not on dual-source RF excitation maps. When evaluating location specific  $B_1$  values, we noted that improvements in  $B_1$  homogeneity were greatest in the central, medial, and posterior aspects of the breasts.

However, we did note that there was significant right-to-left  $B_1$  inhomogeneity on dual-source RF excitation  $B_1$  maps at the anterior location that was not significant on the single-source maps. The reason for this is unclear but could demonstrate that the dual-source method is only able to correct low-order spatial variations in  $B_1$ . Higher channel parallel RF excitation techniques may further improve  $B_1$  homogeneity for breast imaging. Additional investigation into this phenomenon is warranted.

Our results confirm quantitatively the  $B_1$  inhomogeneity challenges that have been previously described (1,2). Prior authors have reported that tissue signal variability due to reduced  $B_1$  occurred most prominently in the right breast while we observed this phenomenon affecting the left breast. This difference is readily explained by patient positioning; the 16-channel coil used for our study enables us to scan patients oriented feet first rather than head first (as was utilized by Azlan et al and Kuhl et al).

Our study has several limitations. We evaluated a small number of patients (n=14), and future larger studies would be useful to confirm our results. However, our results agree with those of previous reports for body MR applications demonstrating improved  $B_1$  homogeneity with dual-source parallel RF excitation (6). Additionally, we sought only to evaluate quantitative differences in  $B_1$  homogeneity; we did not qualitatively assess the appearance of corresponding T1-weighted and T2-weighted images or the effect of  $B_1$  inhomogeneity on clinical interpretation. Finally, as our study was performed on a single 3T Philips MR scanner, our results of improved  $B_1$  homogeneity using dual-source parallel excitation may be vendor specific.

In conclusion, our study confirms that dual-source parallel excitation can significantly improve  $B_1$  homogeneity over conventional single-source excitation techniques in breast MRI at 3T. This technique has the potential to substantially reduce a major challenge of breast MRI at higher field strength and improve tissue contrast and lesion conspicuity.

## Acknowledgments

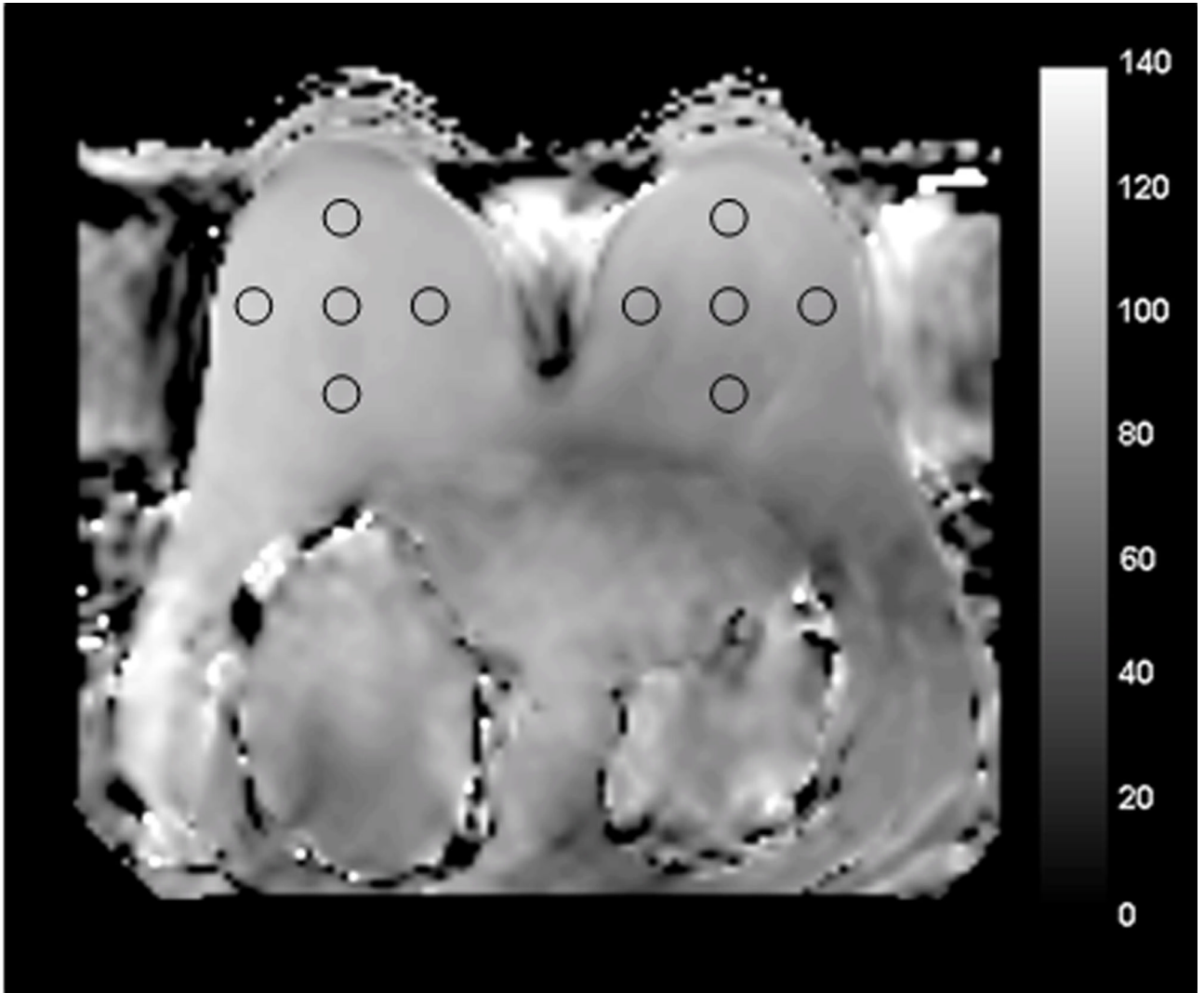
The authors would like to acknowledge our talented MRI technologists, [BLINDED], for their dedicated technical assistance.

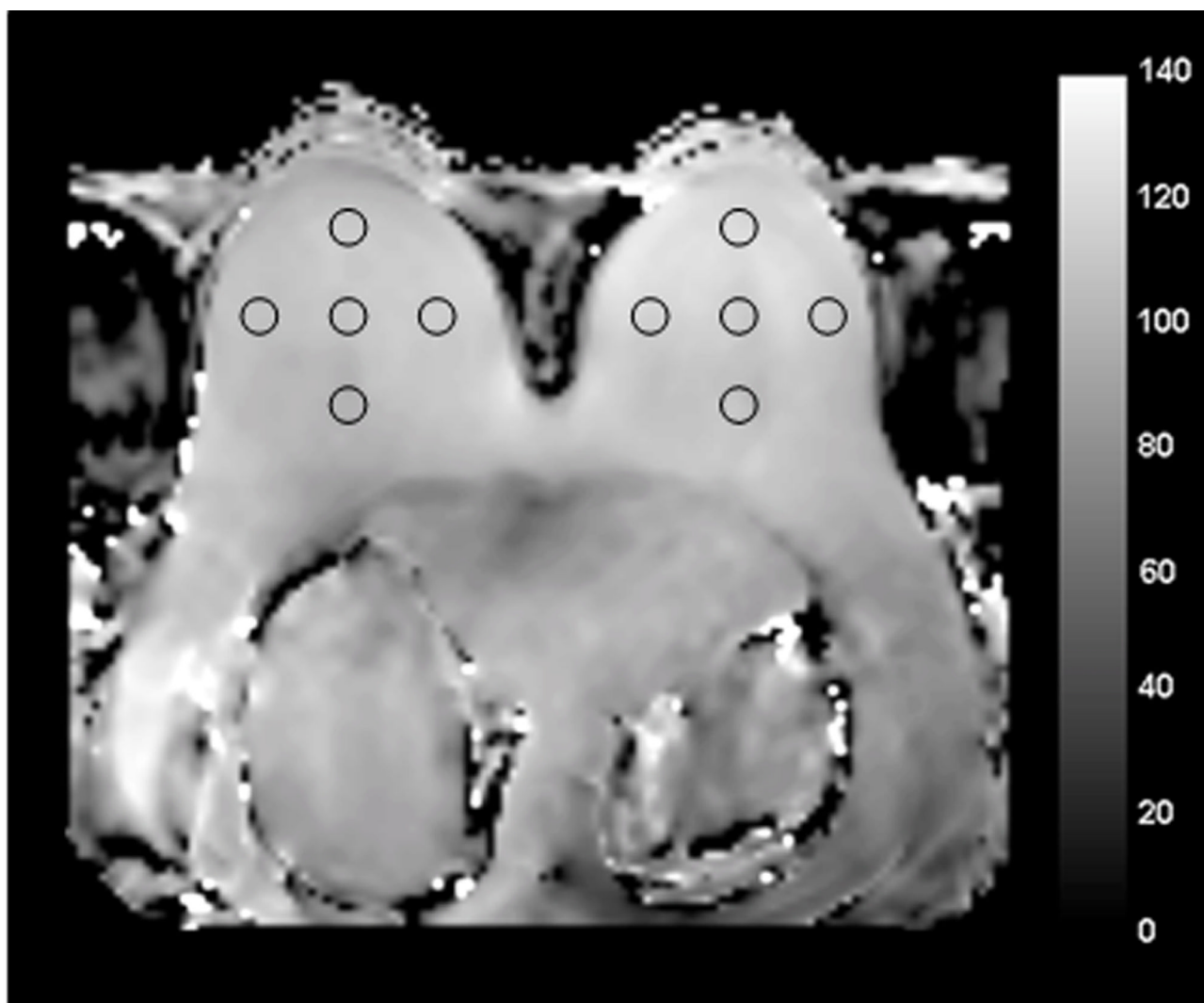
Funding Support: NIH Grant RO1CA151326

## References

1. Kuhl CK, Kooijman H, Gieseke J, Schild HH. Effect of  $B_1$  inhomogeneity on breast MR imaging at 3.0 T. *Radiology*. 2007; 244(3):929–930. [PubMed: 17709843]
2. Azlan CA, Di Giovanni P, Ahearn TS, Semple SI, Gilbert FJ, Redpath TW.  $B_1$  transmission-field inhomogeneity and enhancement ratio errors in dynamic contrast-enhanced MRI (DCE-MRI) of the breast at 3T. *J Magn Reson Imaging*. 2010; 31(1):234–239. [PubMed: 20027594]
3. Rakow-Penner R, Hargreaves BA, Glover GH, Daniel B. Breast MRI at 3T. *Applied Radiology*. 2009; 38(3):6–13.
4. Partridge, SC.; Rahbar, H.; Lehman, CD. Breast MR imaging. In: Kamel, IR.; Merkle, EM., editors. *Body MR Imaging at 3 Tesla*. Cambridge University Press; 2011. p. 26-33.
5. Nelles M, Konig RS, Gieseke J, et al. Dual-source parallel RF transmission for clinical MR imaging of the spine at 3.0 T: intraindividual comparison with conventional single-source transmission. *Radiology*. 2010; 257(3):743–753. [PubMed: 20858848]
6. Willinek WA, Gieseke J, Kukuk GM, et al. Dual-source parallel radiofrequency excitation body MR imaging compared with standard MR imaging at 3.0 T: initial clinical experience. *Radiology*. 2010; 256(3):966–975. [PubMed: 20720078]
7. Yarnykh VL. Actual flip-angle imaging in the pulsed steady state: a method for rapid three-dimensional mapping of the transmitted radiofrequency field. *Magn Reson Med*. 2007; 57(1):192–200. [PubMed: 17191242]
8. Katscher U, Bornert P. Parallel RF transmission in MRI. *NMR Biomed*. 2006; 19(3):393–400. [PubMed: 16705630]
9. Ullmann P, Junge S, Wick M, Seifert F, Ruhm W, Hennig J. Experimental analysis of parallel excitation using dedicated coil setups and simultaneous RF transmission on multiple channels. *Magn Reson Med*. 2005; 54(4):994–1001. [PubMed: 16155886]
10. Vernickel P, Roschmann P, Findekklee C, et al. Eight-channel transmit/receive body MRI coil at 3T. *Magn Reson Med*. 2007; 58(2):381–389. [PubMed: 17654592]

**a**



**b**

**Figure 1.**  
Example of regions of interest (ROIs) drawn at the level of the nipple on the  $B_1$  maps acquired with standard single-source RF excitation (A) and with dual-source parallel RF excitation (B).

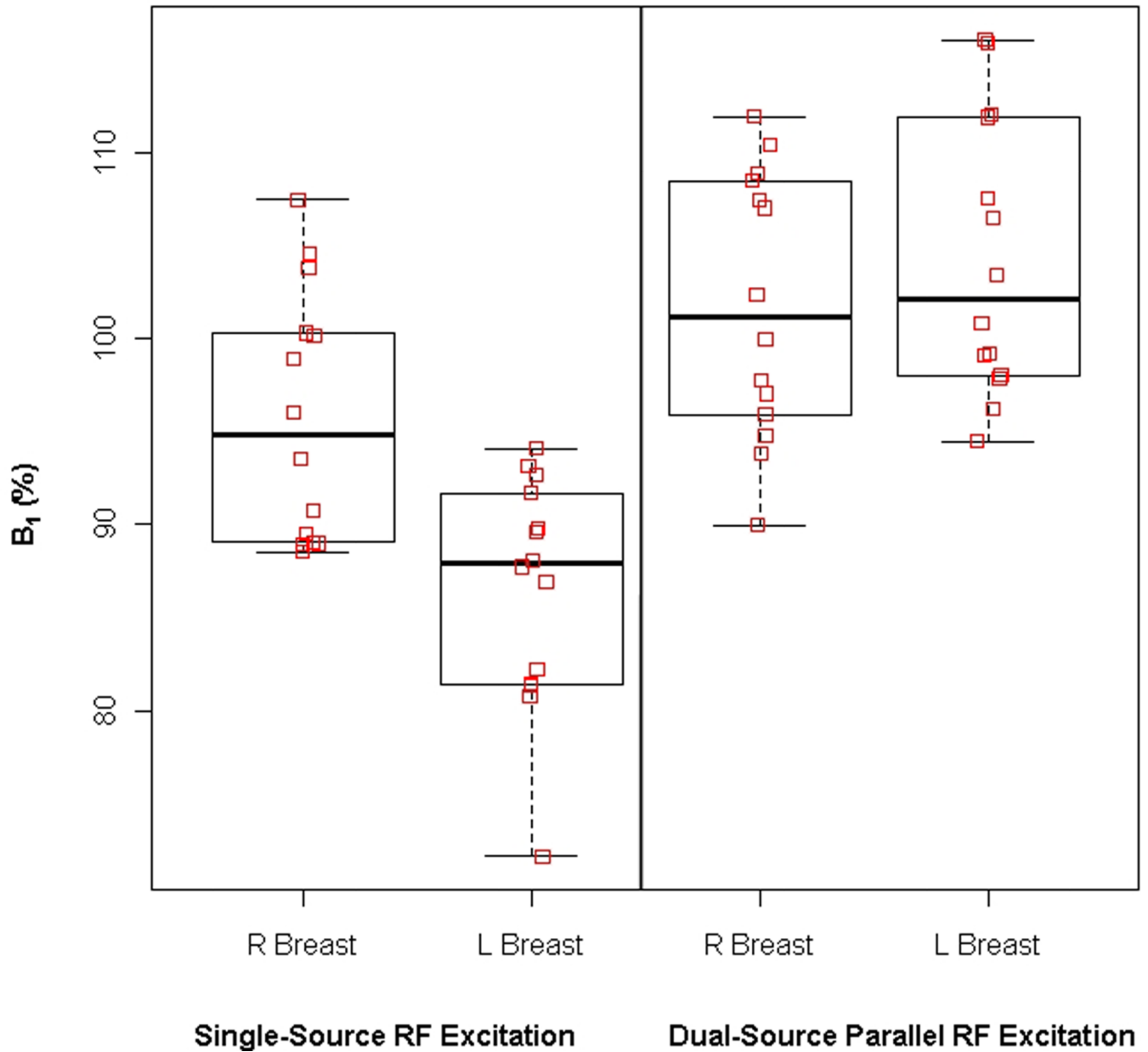
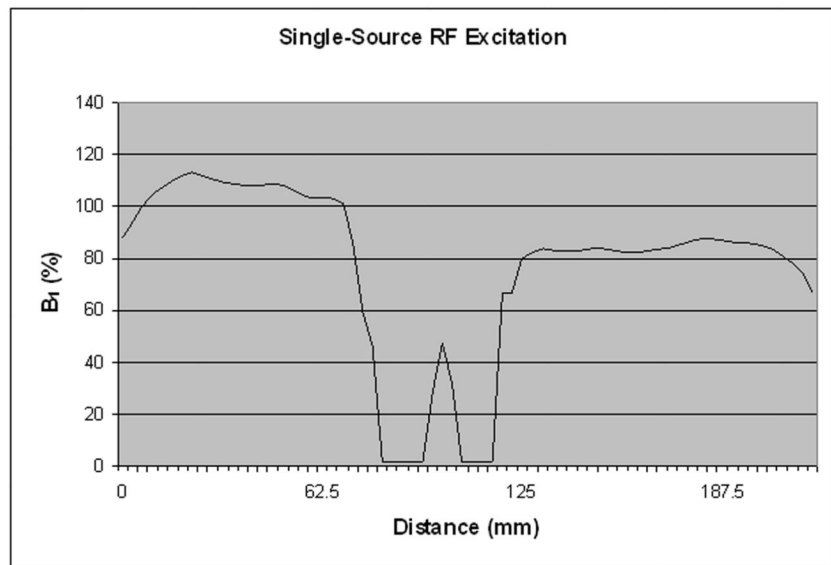
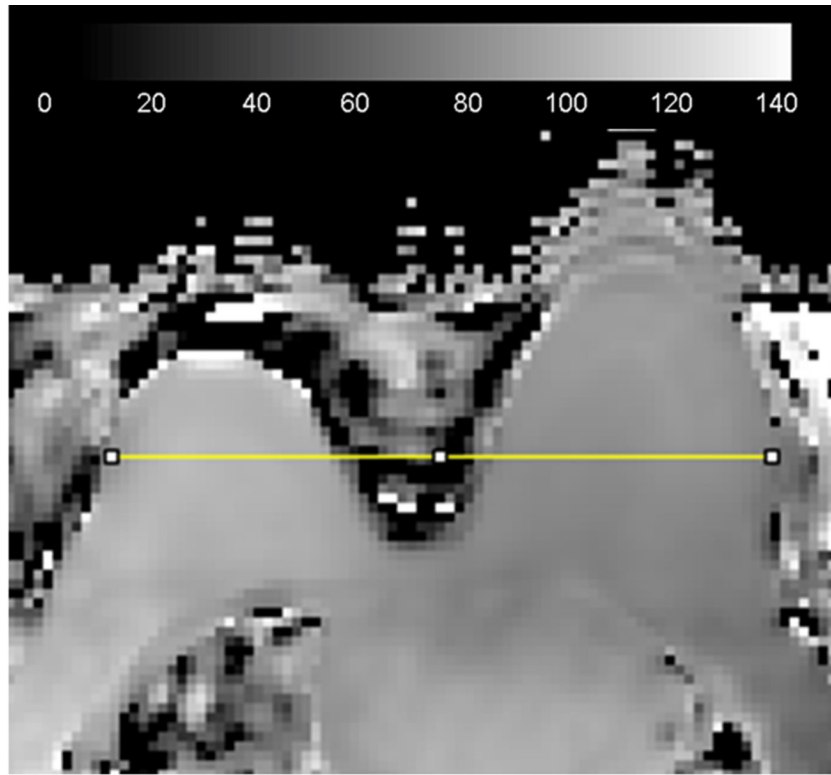


**Figure 2.**

Box plots demonstrating the mean  $B_1$  signal (% of intended  $B_1$ ) and standard deviations between the right and left breasts for all patients in the study. Whole breast  $B_1$  signal significantly differed between right and left breast with single-source RF excitation. However, there was no statistically difference in whole breast  $B_1$  signal with dual-source parallel RF excitation.



**a**



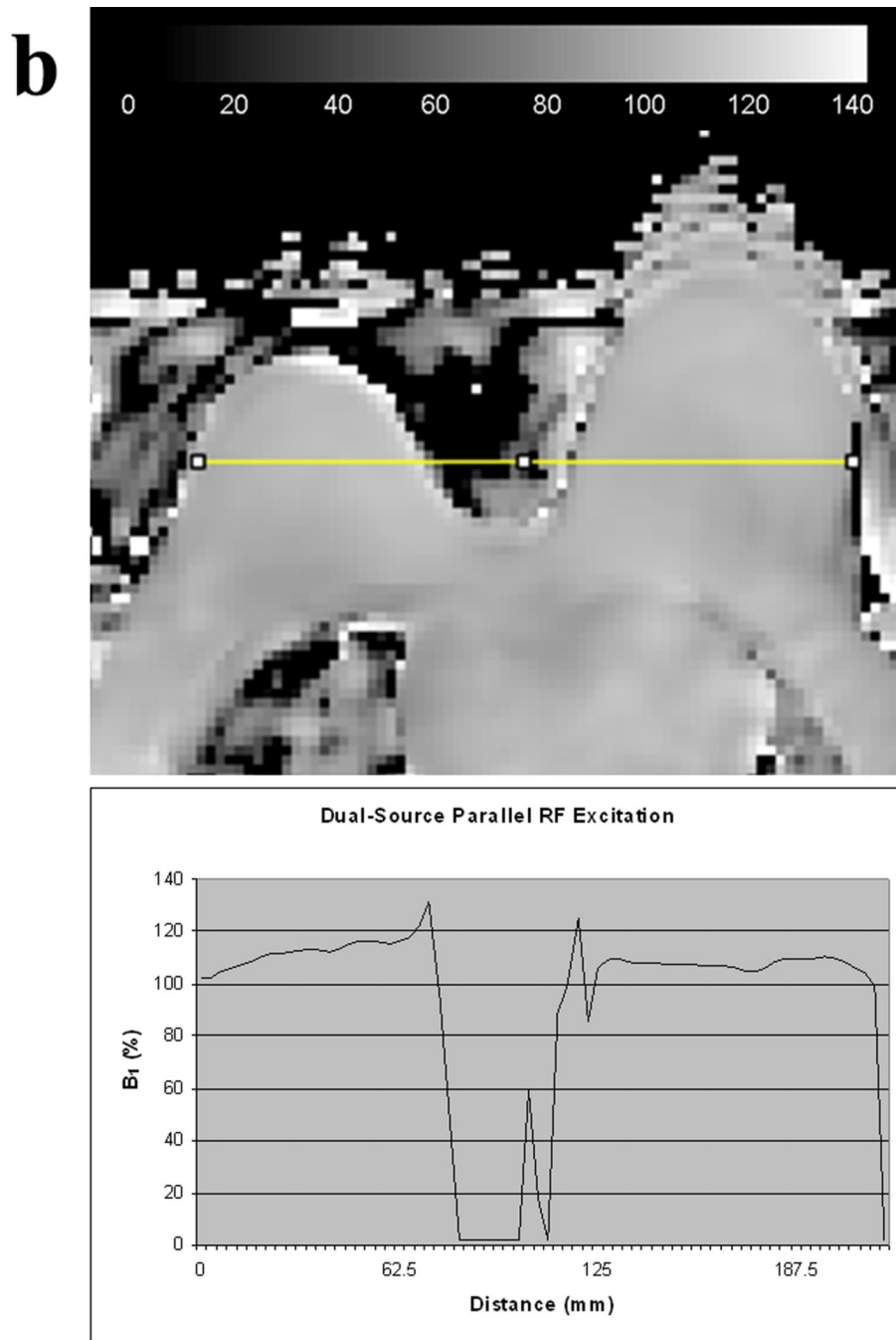


**Figure 3.** B<sub>1</sub> homogeneity between the right and left breasts in the same patient obtained with conventional single-source RF excitation (A) and dual-source parallel RF excitation (B) techniques. Note that both visually and quantitatively, there is a significant decrease in B<sub>1</sub> signal intensity in the left breast with single-source RF excitation whereas a more homogeneous B<sub>1</sub> signal is obtained across the breasts with dual-source parallel RF excitation technique.

Table 1

Mean region-specific B<sub>1</sub> values (% of intended B<sub>1</sub>) for single-source RF excitation and dual-source parallel RF excitation techniques.

ROI Location	Single-Source RF Excitation				Dual-Source Parallel RF Excitation			
	Right (%)	Left (%)	Difference (%)	P value	Right (%)	Left (%)	Difference (%)	P value
Anterior	97.99±8.50	94.15±7.15	-3.83±7.92	0.094	103.99±8.31	108.76±8.64	4.77±7.32	0.030*
Lateral	96.12±8.37	87.84±6.14	-8.28±10.86	0.014*	99.86±5.41	107.39±6.73	7.52±5.67	0.0003*
Central	96.3±7.19	85.34±7.36	-10.95±7.93	0.0001*	102.82±8.60	102.06±8.94	-0.76±6.51	0.668
Medial	96.13±7.62	87.01±7.52	-9.11±8.36	0.0013*	105.24±9.89	104.96±8.33	-0.29±8.12	0.897
Posterior	92.36±8.07	78.37±6.70	-13.99±9.02	<0.0001*	97.45±7.56	98.16±8.66	0.71±7.50	0.727
Whole Breast	95.78±6.74	86.55±6.22	-9.23±6.93	0.0002*	101.87±7.14	104.27±7.42	2.39±4.81	0.085

Abbreviations:

ROI=region of interest

Statistical analysis: two tailed, paired student t test

\* Statistically significant